ELSEVIER

Journal of Nuclear Materials 266–269 (1999) 146–152

journal of nuclear materials

Plasma wall interaction during long pulse operation in Tore Supra

C. Grisolia *, the Tore Supra team

Association Euratom–CEA, Departement de Recherches sur la Fusion Controlée, Centre d'Etudes Nucleaires de Cadarache, F-13108 Saint Paul lez Durance cedex, France

Abstract

Increase of plasma density observed during long pulse operation is reported. The higher the injected and radiated energies are, the faster the increase of density appears. This behaviour correlated with oxygen and hydrogen plasma density increase is attributed to water desorption induced by wall heating due to the high radiated energy of the plasma. These surfaces are far from plasma and are not baked during the conditioning procedures usually used at Tore Supra. Conditioning evidence is seen during discharge series at high injected energy. But this improvement is prevented if disruptions occur in between.

Keywords: Carbon; Chemical erosion; Graphite; Hydrogen; Oxygen; Ion Bombardment

1. Long discharge operation description

Tore Supra is a tokamak in which long discharge operation, e.g., up to 2 min in almost steady-state conditions can be achieved. Limiter and Ergodic Divertor (ED) configurations have been used to perform these long pulses.

In the limiter configuration, the plasma is lying on the inner wall of the machine (10 m^2 of carbon). Very long deuterium discharges [1] are achieved implying a loop voltage almost equal to zero. Plasma volume average density is low ($\langle n_e \rangle = 10^{19}$ m^{-3}) and plasma current is equal to 0.8 MA (ohmic power (P_{ohm}) = 150 kW). The noninductive current is driven by lower hybrid waves (LHCD) at relatively low heating power (~2.2 MW) allowing for time duration up to 120 s. Indeed, I_{CD}, the current generated by LHCD can be expressed by:

$$I_{CD} = \eta_{CD} \frac{P_{LH}}{\langle n_e \rangle R}, \quad (1)$$

where P_{LH} is the lower hybrid injected power, η_{CD} is the current drive efficiency and R the plasma radius. The available P_{LH} allows a decrease of the loop voltage close to zero only for $\langle n_e \rangle \leqslant 10^{19}$ m^{-3}. The radiated power (Pr) is low (0.6 ~ MW) in such case. An uncontrolled density increase is often observed after a time lag of 60 to 70 s (see Fig. 1). Using this plasma configuration, 15 discharges have been realised at Tore Supra.

Plasmas can also be operated at higher density (up to 2.5×10^{19} m^{-3}) and higher heating power (up to 6.6 MW) combining LH (2 MW), ICRH (4.2 MW) and ohmic power (400 kW). Plasma current is then equal to 1 MA. Due to higher density operation and larger ohmic power, the duration of these D_2 discharges is reduced to 30 s as loop voltage is equal to 0.3 V. Pr is higher in this case (1.5–2 MW). A density increase is observed after 15 s (see Fig. 2).

In the ergodic divertor (ED) configuration [2], the recent upgrading of power exhaust capability allows pulse duration up to 20 s at rather low density (1.6×10^{19} m^{-3}) with higher LHCD power (3.7 MW) [3]. These experiments, despite active pumping and different wall interaction, also exhibit a density increase after 13 s.

In this paper, we will focus on the discharge series realised at high density and high injected energy in the limiter configuration. During the corresponding operational day, a series of four consecutive discharges have been done with high injected energy (more than 150 MJ

* Tel.: +33-442 25 43 78; fax: +33-442 25 62 55; e-mail: grisolia@drfc.cad.cea.fr.

0022-3115/99/$ – see front matter
PII: S0022-3115(98)00815-0

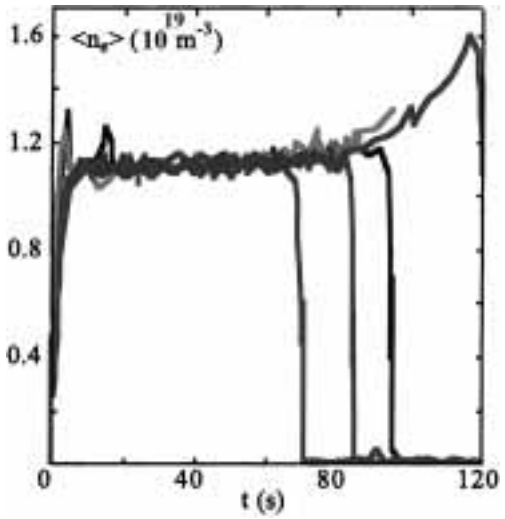

Fig. 1. Volume average density evolution for very long discharges (low injected and radiated energy and low plasma density).

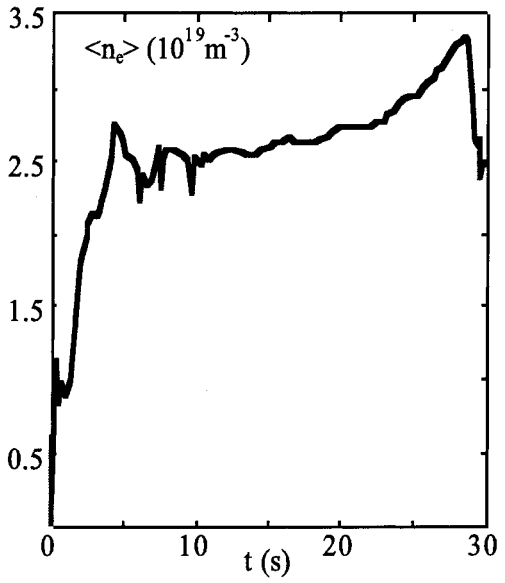

Fig. 2. Volume average density time evolution for a long discharge (high injected and radiated energy and high plasma density).

constant from pulse to pulse) and accordingly high radiated energy (greater than 45 MJ). This gives the opportunity to follow the plasma wall interaction evolution from pulse to pulse.

After a rapid review of long pulse possible limitations (part II), experimental results will be presented (part III and IV). Then using a multi machine scaling law [4] and experimental signals, plasma composition will be deduced (part V). Finally, a conditioning improvement from pulse to pulse will be presented (part VI).

2. Long discharge limitations

The time duration of long pulse can be constrained by various processes. The first one is a degradation of the first wall interacting with high plasma fluxes. This was observed in the past at Tore Supra when pieces of carbon tile were broken during the discharge and then penetrated into the plasma edge leading immediately to a plasma collapse. This catastrophic behaviour has almost completely disappeared due to a partial upgrade of the plasma interacting inner wall which is now composed of carbon fiber composite tiles instead of graphite ones with a better brazing technology [5].

Another possible effect leading to a reduced pulse duration is wall damage due to ripple trapped electrons or to localised deposition of a large energy flux on very small interacting surfaces due to electrons accelerated by the electric field in the vicinity of LH grill. While the former effect should be reduced by the density rise, the second one is amplified by the increase of the boundary density [3,6]. However, these two limiting behaviours can be effectively reduced by using a sweeping of the plasma current which spreads the localised energy fluxes.

In these partial noninductive current drive discharges, plasma current I_p is the sum of an inductive part (I_Ω) and of noninductive one I_{CD}:

$$I_p = I_{CD} + I_\Omega. \tag{2}$$

From Eq. (1):

$$I_p = \frac{\eta_{CD}}{\langle n_e \rangle}\frac{P_{LH}}{R} + \frac{V_{loop}}{\rho}, \tag{3}$$

where V_{loop} is the plasma loop voltage and ρ is the mean plasma resistivity ($\rho \propto T_e^{-1.5}$).

$$\delta I_p = \left(\frac{\delta\eta_{CD}}{\eta_{CD}} - \frac{\delta\langle n_e\rangle}{\langle n_e\rangle} + \frac{\delta P_{LH}}{P_{LH}}\right) I_{CD} + \left(\frac{\delta V_{loop}}{V_{loop}} - \frac{\delta\rho}{\rho}\right) I_{loop}. \tag{4}$$

$\eta_{CD} = f(T_e)$ and $\langle n_e\rangle T_e \propto P_{tot}\tau_E$ where P_{tot} is total plasma stored energy and τ_E is energy confinement time. Assuming that $P_{tot}\tau_E$ is constant, the following expression results:

$$\delta I_p = \left(-2\frac{\delta\langle n_e\rangle}{\langle n_e\rangle} + \frac{\delta P_{LH}}{P_{LH}}\right) I_{CD} + \left(\frac{\delta V_{loop}}{V_{loop}} - \frac{3}{2}\frac{\delta\langle n_e\rangle}{\langle n_e\rangle}\right) I_{loop}. \tag{5}$$

Therefore, if $\langle n_e\rangle$ increases, P_{LH} has to be increased to maintain I_p constant ($\delta I_p = 0$). However, this compensation is limited by the amount of P_{LH} available on the

tokamak. Thus, an increase of $\langle n_e \rangle$ will lead to a lowering of the current driven by LH power and in turn to an increase of the magnetic flux consumption to maintain plasma current constant. Moreover, the inductive part of I_p is also sensitive to any density rise and an increase of $\langle n_e \rangle$ will lead to greater flux consumption. As a consequence, plasma duration is shortened by any density rise.

Therefore it appears that steady-state operation in long pulses which are done with lower hybrid current drive requires control of any density excursion.

3. Density increase and wall saturation

The wall saturation status is routinely estimated at Tore Supra through a special procedure which occurs during the start of the premagnetization phase of the discharge when the poloidal coils are energised [7]. Plasma tests are obtained. They are realised with D_2 prefill and with wall fuelling. Plasma experiences no poloidal control and Vloop is constant. In Fig. 3(a), time traces of two plasma currents are plotted. The difference in the shape of these small plasma currents come from distinct wall saturation status. When the mean value of plasma current is plotted against its integrated value for a great series of 800 plasmas tests, the diagram presented in Fig. 3(b) is obtained. Every point on this diagram represents a plasma test. All the characteristic points are lying along a trajectory from desaturated wall conditions (point A) to a saturated one (point B). The level of desaturation is determined by a nondimensional desaturation parameter (K_s). It is calculated from the position of a plasma test characteristic point with regard to a centre of rotation (point C). K_s is varying from 1000 corresponding to desaturated conditions (point A) to 0 which stands for saturated values (point B). The values of K_s are not linear with the position around C but calculation emphasises the regions between intermediate wall saturation (point D) and saturated wall conditions (point B). If K_s is greater than 600, walls are considered as desaturated. In contrary, if K_s is less than 100, walls are saturated and current ramp up becomes impossible due to an early radiation collapse. For the two pulses of Fig. 3(a), $K_s = 950$ for desaturated conditions and $K_s = 400$ for intermediate wall saturation conditions. Therefore, this procedure gives an estimation of the saturation status of the walls just before the start up of the discharge.

In Fig. 4, K_s is presented for a series of six consecutive high density – high energy pulses which are the subject of this study. Discharge 23868 ends by a disruption. This causes a real diminution of K_s determined just before the beginning of the following discharge (23869). However, during the next discharges as for 23868, K_s is always greater than 600. Therefore, no evidence of wall saturation during these long discharge operation is observed. Calculations done by Federici and Sugihara on long pulse low density operation [8,9]

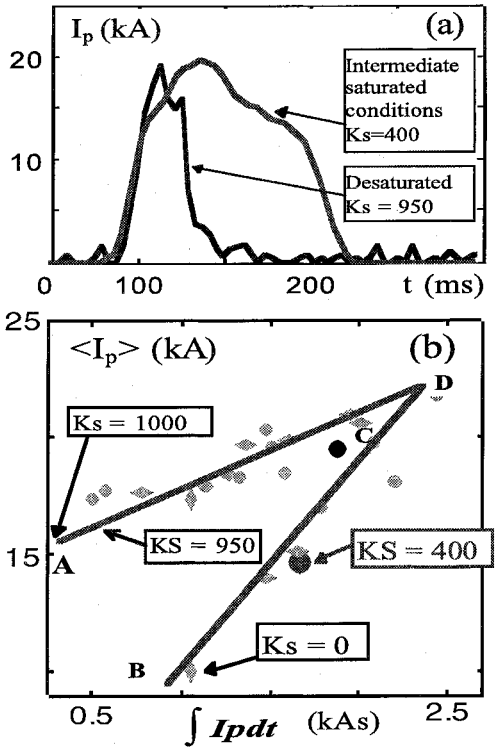

Fig. 3. (a) Plasma current obtained in premagnetisation phase for nonsaturated and saturated wall. (b) Desaturation diagram. $K_s = 1000$ corresponds to a deep desaturated wall while $K_s < 100$ is the signature of a completely saturated wall. Point A: desaturated wall, point B: saturated wall. Point C: "center of rotation". All the characteristic points (more than 800) are lying around the two trajectories.

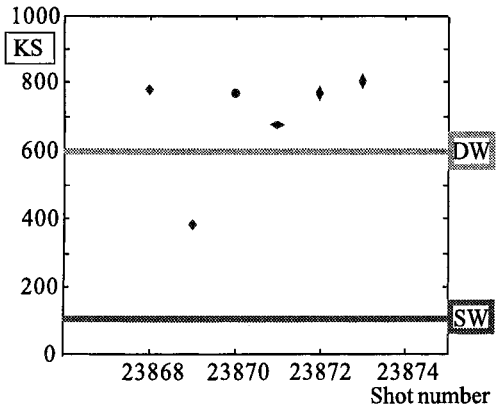

Fig. 4. Desaturation parameter (K_s) evolution for a given discharge series. DW: desaturated wall and SW: saturated walls.

lead to the same conclusion for very long pulse operation: to fit the observed density evolution, no wall saturation hypothesis is needed.

4. Density increase and intrinsic impurities behaviour

In Fig. 5, time traces of C_{VI} brightness and I_p are plotted in part a and $\langle n_e \rangle$ and O_{VIII} brightness in part b. Here, I_p is modulated to spread the localised energy flux onto actively cooled wall components. C_{VI} follows the same modulation as I_p and decreases after 20 s of discharge operation. To the contrary, O_{VIII} is not modulated and increases with $\langle n_e \rangle$ after 20 s. These two different time evolutions for C_{VI} and O_{VIII} are indicative of two distinct generation processes for these intrinsic plasma impurities.

In Fig. 6, time traces of H_α and C_{VI} are plotted. The H_α line of sight is an equatorial plane chord viewing the inner wall where the plasma is lying. H_α and C_{VI} decrease similarly after 20 s. This behaviour, correlated with an increase of the radiated power, is probably due to a decrease of plasma heat flux and consequently of the electron temperature. This observation suggests that carbon source is mainly due to physical sputtering. On the contrary, the oxygen source is expected to originate from remote surfaces far from plasma wetted zones. This point is discussed in Section 5.

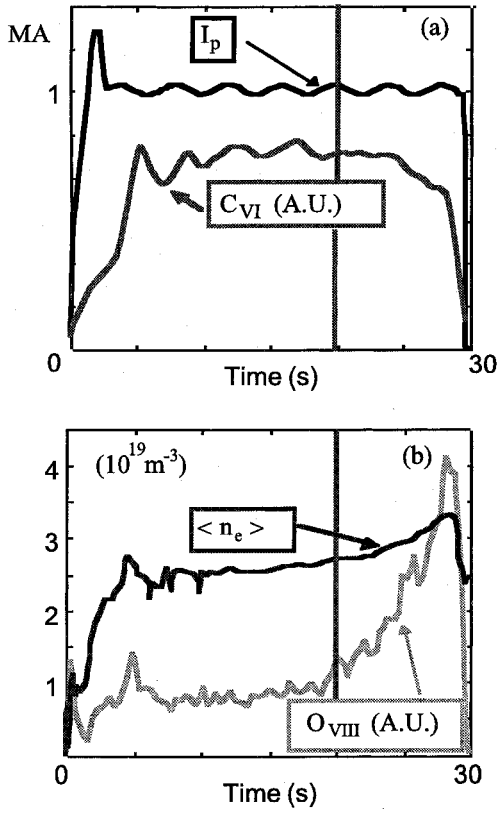

Fig. 5. (a) Plasma current (I_p) and C_{VI} brightness time evolution for a typical discharge analyzed (23869). (b) Volume average density ($\langle n_e \rangle$) and O_{VIII} brightness for the same discharge.

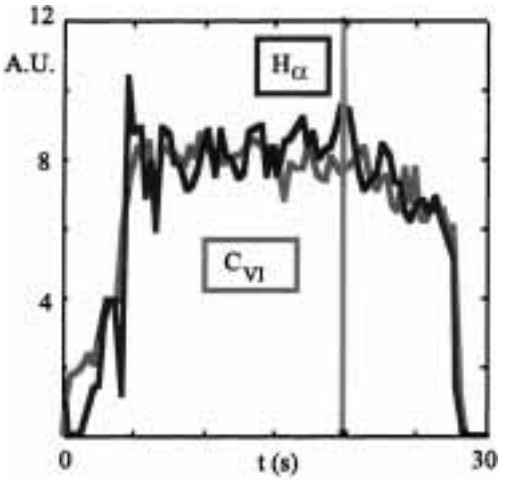

Fig. 6. Time traces of C_{VI} and H_α measurements for the same discharge as Fig. 5.

The observed plasma isotopic ratio ($n_H/n_H + n_D$) is displayed in Fig. 7(a). It is deduced from high energy charge exchange measurements. It is increasing continuously during the discharge. This is due to an influx of hydrogen during the discharge. This result is confirmed (see Fig. 7(b)) by mass spectrometry measurements of the gas outflux in the pumping system of Tore Supra. These are done far from the plasma edge. Partial pressure of HD (P_{HD}) and H_2 (P_{H_2}) are increasing whereas partial pressure of D_2 (P_{D_2}) stays constant until almost the end of the discharge. P_{CO}, which is the partial pressure of CO and characterises the presence of water or oxygen around the plasma is increasing in the same way as P_{H_2}.

5. Experimental analysis

The experimental results will be analysed in the frame of the multi machine scaling law which links the radiated power (Pr) to the average effective plasma charge Z_{eff} [4]. For Tore Supra, the following expression is obtained for Pr:

$$\mathrm{Pr} = 10^{-39}(Z_{\mathrm{eff}} - 1)\langle n_e \rangle^2. \quad (6)$$

The only significant impurities observed in the analysed discharges are carbon and oxygen. Therefore, the expressions for Z_{eff} and $\langle n_e \rangle$ are

$$(Z_{\mathrm{eff}} - 1)\langle n_e \rangle = 56\langle n_O \rangle + 30\langle n_C \rangle, \quad (7)$$

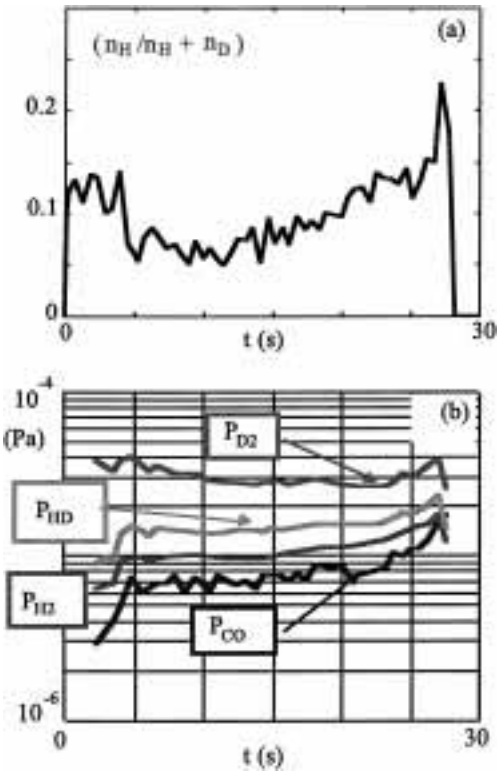

Fig. 7. (a) Time evolution of the isotopic plasma ratio for the same discharge as Fig. 5 (from CX measurements). (b) Partial pressure measured by RGA on the gas outflow to the pumps.

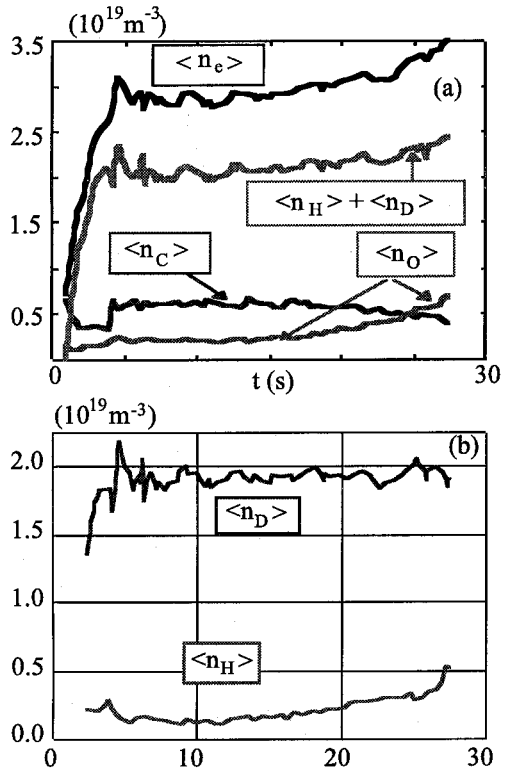

Fig. 8. (a) Plasma composition during long discharge operation (high injected and radiated energy – high density). (b) Time evolution of H and D density in the same discharge.

$$\langle n_e\rangle = (\langle n_H\rangle + \langle n_D\rangle) + 8\langle n_O\rangle + 6\langle n_C\rangle, \tag{8}$$

where $\langle n_O\rangle$ and $\langle n_C\rangle$ represent the density of oxygen and carbon and $\langle n_D\rangle$ and $\langle n_H\rangle$ the density of deuterium and hydrogen.

Pr and $\langle n_e\rangle$ are taken from experimental results and time evolution of Z_{eff} is obtained with the help of Eq. (6).

Due to similar spontaneous emission probabilities of O_{VIII} and C_{VI} measured by a grazing incidence X-UV spectrometer, the density ratio of oxygen and carbon is assumed to be equal to the brightness ratio of these intrinsic impurities:

$$\frac{\langle n_O\rangle}{\langle n_H\rangle} = \frac{O_{VIII}}{C_{VI}}. \tag{9}$$

Thus, plasma composition can be estimated and the result is given on Fig. 8(a). In this graph, $\langle n_O\rangle$ and $\langle n_C\rangle$ appear together with $(\langle n_H\rangle + \langle n_D\rangle)$.

From this estimation of $(\langle n_D\rangle + \langle n_H\rangle)$ and using the plasma isotopic ratio measurements, time evolution of $\langle n_H\rangle$ and $\langle n_D\rangle$ are calculated (see Fig. 8(b)). $\langle n_D\rangle$ is constant during all the discharge whereas $\langle n_H\rangle$ is increasing from $t = 10$ s.

In this plasma for which radiated energy is high (more than 45 MJ), the increase of plasma density is attributed to an increase of oxygen and hydrogen plasma density. Deuterium density remains constant for all the pulse duration whereas carbon density tends to decrease after 20 s. This suggests that the drive mechanism for the density increase is thermal desorption of water coming from cold surfaces distant from plasma and heated by radiated energy. These remote wall parts could be stainless steel surfaces of the Tore Supra ports. They cannot reach the vessel baking temperature used during conditioning procedures ($T_w \sim 200$°C). They are only heated to higher temperature during high radiated plasmas.

The increase of temperature (ΔT) of distant walls can be estimated using a semi-infinite wall model:

$$\Delta T \propto \Phi_r t^{0.5}, \tag{10}$$

where Φ_r is the radiated flux impinging the surface and t is the time.

In the case of stainless steel surface placed in a port and heated by 10 kW/m^2 radiated power (depth of wall 5 cm, 100 s of interaction), $\Delta T \sim 20$°C. During conditioning procedure, an identical increase of wall baking temperature leads to an increase of CO production measured by mass spectrometry by at least a factor of 2.

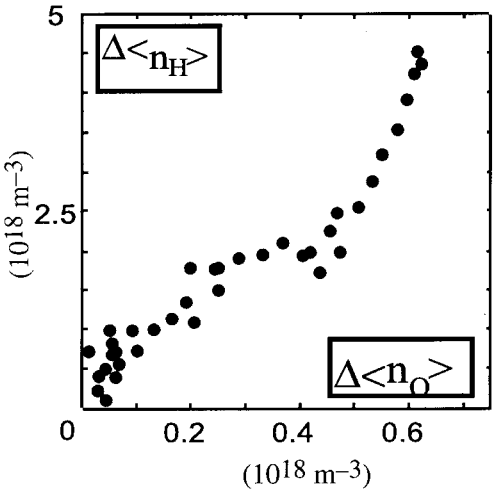

Fig. 9. Hydrogen atoms density increase ($\Delta\langle n_H\rangle$) against oxygen atoms density increase ($\Delta\langle n_O\rangle$) in a given discharge (23869). $\Delta\langle n_H\rangle/\Delta\langle n_O\rangle \propto 6$.

($T_{initial} \sim 150$°C). This CO production can be much higher in the case of nonbaked surfaces which could be at almost ambient temperature and which act as water traps.

An estimation of the increase of the H (ΔH) and O (ΔO) atoms in the plasma due to water desorption is deduced from plasma composition. At any time $t > 10$ s

$$\Delta\langle n_H\rangle = \langle n_H(t)\rangle/\langle n_H(t = 10\text{ s})\rangle$$

(same estimation for ΔO).

Time $t = 10$ s is taken as a reference time because $\langle n_H\rangle$ and $\langle n_O\rangle$ are only increasing afterwards. A plot of $\Delta\langle n_H\rangle$ versus $\Delta\langle n_O\rangle$ is shown in Fig. 9 for a given discharge. $\Delta\langle n_H\rangle/\Delta\langle n_O\rangle \approx 6$ is an estimation of the relative screening efficiency of oxygen compared to hydrogen for a source of water.

6. Conditioning improvement from pulse to pulse

The time evolution of the density for a given discharge is plotted in Fig. 10(a). To investigate any "conditioning" improvement from pulse to pulse, the difference between the maximum density reached at the end of a discharge and the density at $t = 10$ s ($\Delta\langle n_e\rangle$) is taken as a criterion. The evolution of $\Delta\langle n_e\rangle$ is given in Fig. 10(b) for a series of successive discharges. During the first four discharges of this series, $\Delta\langle n_e\rangle$ decreases strongly by a factor of four showing that repeating high radiated energy discharges substantially reduces the water desorption. Therefore, a net conditioning improvement is found.

Unfortunately, technical problems occurring during discharge 23874 lead to a great plasma disruption. Then

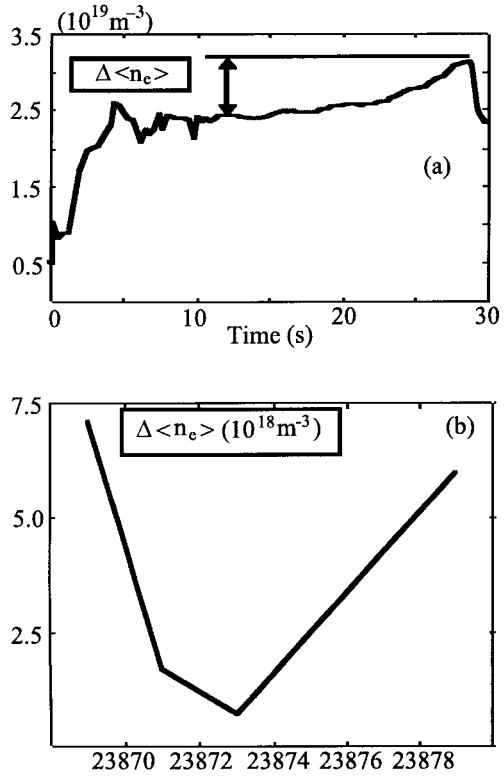

Fig. 10. (a) Time evolution of the density. $\Delta\langle n_e\rangle$, maximum increase of the density, criterion of conditioning improvement. (b) $\Delta\langle n_e\rangle$ evolution for a series of discharge.

four discharges were necessary to recover good enough plasma operation to run again a plasma with the same discharge configuration as 23873 in which more than 150 MJ of total energy were coupled. In this case (discharge 23879), $\Delta\langle n_e\rangle$ is again very high showing net deconditioning effects after these noncontrolled operations. This is probably due to water and/or oxygen production during disruption which are then trapped again in cold surfaces far from plasma before reaching the turbomolecular pumps of Tore Supra. It appears clearly that this water retrapping has to be avoided in future fusion devices. That is why, in the framework of the CIEL project [10] which is a Tore Supra upgrade, a complete coverage of the vessel and ports by actively cooled panels at a temperature up to 230°C is contemplated.

7. Conclusions

In this paper, increase of plasma density observed during long discharge plasma operation is reported. The higher the injected and radiated energies are, the faster the increase of density appears. This behaviour cannot

be correlated with any wall saturation. It originates from water desorption induced by wall heating due to the high radiated energy of the plasma. These surfaces are far from plasma and are not baked enough during the conditioning procedures usually used at Tore Supra.

The evolution of the density increase during a discharge is an avalanche phenomenon. Indeed, the increase of the oxygen in the discharge leads to an increase of the radiated energy. This implies an increase of the water desorption and of the oxygen in the plasma, etc.

Conditioning improvement is found during a series of discharges at high injected energy. But this betterment can be easily deteriorated in the case of disruptions.

To avoid such a density increase, water recirculation has to be controlled by preventing any gradient of baking temperature all around the vessel. This baking temperature has to correspond to the highest temperature reached during plasma operation. Moreover, a cold temperature point may be used as a trap of water. Its implementation can be envisaged.

The increase of the density occurs after 60–70 s for low density-low radiated energy discharges and after 15 s for higher density-higher radiated energy discharges. If this type of behaviour is kept for short pulse high density operation, an increase of $\langle n_e \rangle$ will be observed after less than 1 s for 15 MW of injected energy. To the contrary, for 1000 s discharge operation done at low density, radiated power has to be maintained as low as 0.1 MW. Such condition is not relevant for tokamak operation and an upgrade of Tore Supra wall elements (the CIEL project) is to be installed within 2 years to insure a temperature control of all surfaces subject to any heat flux streaming from the plasma.

References

[1] D. Van Houtte, Equipe Tore Supra, Nucl. Fusion 33 (1993) 137.
[2] A. Grosman et al., J. Nucl. Mater. 241–243 (1997) 532.
[3] I. Pugno et al., these Proceedings.
[4] G. Matthews et al., J. Nucl. Mater. 241–243 (1997) 450.
[5] Equipe TORE-SUPRA, Fusion Technology 29 (1196) 417.
[6] J.H. Harris et al., J. Nucl. Mater. 241–243 (1997) 511.
[7] C. Grisolia et al., J. Nucl. Mater. 241–243 (1997) 538.
[8] M. Sugihara et al., Contr. Fusion and Plasma Phys., European Physical Society 3 (1993) 997.
[9] M. Sugihara et al., these Proceedings.
[10] M. Lipa et al., in: Proceedings of the 17th Symposium on Fusion Engineering, to be published.